NRIAG Journal of Astronomy and Geophysics (2016) 5, 380–392

National Research Institute of Astronomy and Geophysics

NRIAG Journal of Astronomy and Geophysics

www.elsevier.com/locate/nrjag

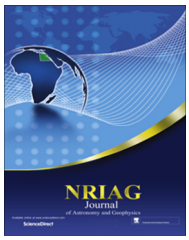

FULL LENGTH ARTICLE

Inferring the subsurface basement depth and the structural trends as deduced from aeromagnetic data at West Beni Suef area, Western Desert, Egypt

Ahmed Khalil [a,*], **Tharwat H. Abdel Hafeez** [b], **Hassan S. Saleh** [b], **Waheed H. Mohamed** [b]

[a] *National Research Institute of Astronomy and Geophysics (NRIAG), 11421 Helwan, Cairo, Egypt*
[b] *Geology Dept., Faculty of Science, Al-Azhar University, Cairo, Egypt*

Received 15 June 2016; revised 8 August 2016; accepted 8 August 2016
Available online 23 August 2016

KEYWORDS

Aeromagnetic;
RTP;
2-D modeling and Euler deconvolution

Abstract The present work aimed to delineate the subsurface structures and to estimate the magnetic source depth at the selected area lying in West Beni Suef area, Western Desert, Egypt, following different geomagnetic techniques. The analysis of aeromagnetic data demonstrates five significant tectonic faults trending to NW-SE, ENE-WSW, NE-SW, E-W and NNW-SSE directions constructed using Euler deconvolution techniques. The execution of this study is initiated by transformation of the total intensity aeromagnetic data to the reduced to pole (RTP) magnetic intensity. This is followed by applying several transformation techniques and various filtering processes through qualitative and quantitative analyses on magnetic data. The reduced to the northern magnetic pole (RTP) data are separated spectrally into regional and residual magnetic components using the computed power spectrum of the magnetic data. The estimated mean depths of both regional and residual sources are found to be 5.27 km and 2.78 km respectively. Also, depth estimations have been conducted by application of the Euler deconvolution and 2-D modeling techniques. The results indicate that the eastern and northern parts of the study area discriminate deeper basement relief and the depth of basement surface reaches to 5095 m. While the southern and western parts of the study area discriminate shallower basement relief and the depth of basement surface

* Corresponding author.
E-mail addresses: ahmedbakr73@hotmail.com, ahmedkhalil68@yahoo.com (A. Khalil).

Peer review under responsibility of National Research Institute of Astronomy and Geophysics.

Production and hosting by Elsevier

http://dx.doi.org/10.1016/j.nrjag.2016.08.001

reaches to 227 m. This study has given a clear picture of the geologic structures beneath the study area.

1. Introduction

Magnetic method represents one of the most useful available tools that help in the recognition of the surface and subsurface geology. The purpose of the application of the aeromagnetic interpretation is to help in solving the problems of regional geological mapping and structure, delineation of buried contacts, site of the probable areas of rock differentiation, mineralization and thickness of sedimentary cover (Domzalski, 1966). It is also used to delineate the basement depth and the subsurface structures around Beni Suef area. Meshref et al. (1980) analyzed magnetic trends in the northern part of Egypt and stated that the basement rocks in the Western Desert have been affected by two fault systems having large vertical and horizontal displacements. The oldest E-W and ENE faults are intersected by the youngest N-W and NNW. Abu El-Ata (1990), based on seismic and gravity data, outlined three structural highs and two lows:

(a) Abu Roash high that strikes first NNE–SSW and then ENE–WSW.
(b) El-Sagha high which is oriented NW–SE.
(c) El Faras-El Fayoum high that is oriented first ENE–WSW and then NNW–SSW.

Tectonically, the area under consideration is a part of the unstable shelf of North Africa and the Mediterranean region (Said, 1962) and is related to the mobile belt (Weeks, 1952), which is characterized by a complex subsurface structural pattern. It is characterized by major and minor faultings originated by action period of prevailing tensional relief. Many fault trends (E–W, WNW, ENE, NW and NNE) have been deduced from the different geological and geophysical studies, which were carried out by many investigators (e.g., Riad, 1977; Meshref, 1982). A folding system was also recorded in the area as a result of the compression forces.

The area under investigation is located at Beni Suef Governorate in the eastern portion of the northern Western Desert of Egypt, immediately to the southwest of Cairo and situates about 150 km south of Cairo. It is bounded by longitudes 30° 26′ 11″E & 31° 21′ 45″E, and latitude 28° 49′ 33″N & 29° 11′ 12″N (Fig. 1), occupying an area of about 4000 km^2.

2. Lithostratigraphy

The stratigraphic column of the Beni Suef Basin (Fig. 2) represents a part of the Northern Western Desert which extends from the Pre-Cambrian granitic basement through the Jurassic clastics of Eghi Formation followed by the Cretaceous sequence which represents the main stratigraphic column of the study area and up to the Eocene Apollonia carbonates and Oligocene shales of the Dabaa Formation (Zahran et al., 2011). Late Tertiary to recent deposition is also recorded within the ancestral Nile valley and along its margins (Zahran et al., 2011). The Cretaceous sequence is divided into lower units made up primarily of clastics and the upper units made up mainly of carbonates (Hantar, 1990). The Lower Cretaceous sequence is divided into five rock units from bottom to top: Betty, Alam El-Bueib, Alamein, Dahab and Kharita formations, but Alamein Formation may not be deposited or eroded in the study area. Betty Formation consists of a shale bed with sandstone interbeds. Alam El Bueib Formation is represented by a sandstone unit with frequent shale interbeds. Dahab Formation is a shale unit with thin interbeds of siltstone and sandstone. Kharita Formation consists of a fine to course grained sandstone with subordinate shale and carbonate beds. The Upper Cretaceous marks the beginning of a major transgression which resulted in the deposition of a dominantly carbonate section (Said, 1962). The Upper Cretaceous sequence is divided into three rock units from bottom to top: Baharyia, Abu Roash and Khoman (Hantar, 1990). The Baharyia Formation comprises medium- to coarse-grained sandstone with calcareous silty shale interbeds. Abu Roash Formation is divided into seven members designated from bottom to top: G, F, E, D, C, B and A (Said, 1962). Members B, D, and F are relatively clean carbonates whereas members A, C, E and G are largely fine clastics with minor carbonate interbeds. The Khoman Formation consists of chalky limestone which is deposited in open marine outer shelf conditions.

3. Aeromagnetic survey

The studied area was surveyed by Egyptian General Petroleum Cooperation using airborne magnetic, the total magnetic intensity measurements were carried out using the high-sensitivity (0.01 nT) airborne proton free-precision magnetometer (Varian, V-85), mounted in a tail stinger. In addition, the Varian (VIW 2321 G4) single-cell cesium vapor was used as base station magnetometer. The flight lines of the survey were flown along parallel traverse lines in a NE-SW direction, with an azimuth of 45° and 225° from the true north. Meanwhile, the tie lines were flown in a NW-SE direction at right angles to the main flight line direction with an azimuth of 135° and 315° from the true north (Aero-Service, 1984). The traverse flight lines of the studied area were oriented in a northeast-southwest direction at 1.5 km spacing, while the tie lines were flown perpendicularly in a northwest-southeast direction at 5 km intervals. For safety reasons, the flight altitude was 3000 Feet (Aero-Service, 1984). A crystal-controlled time-of-day clock was synchronized to international time signals using a short-wave radio, so that correlation with the airborne data is assured (Aero-Service, 1984). In addition, a micro-processor based digital recording system using a 9-track, 800-BPI tape system and analog display recorded the total magnetic intensity resolved to 0.01 nano-Tesla (nT) at one second intervals during the periods of flight and generally on a 24-h basis.

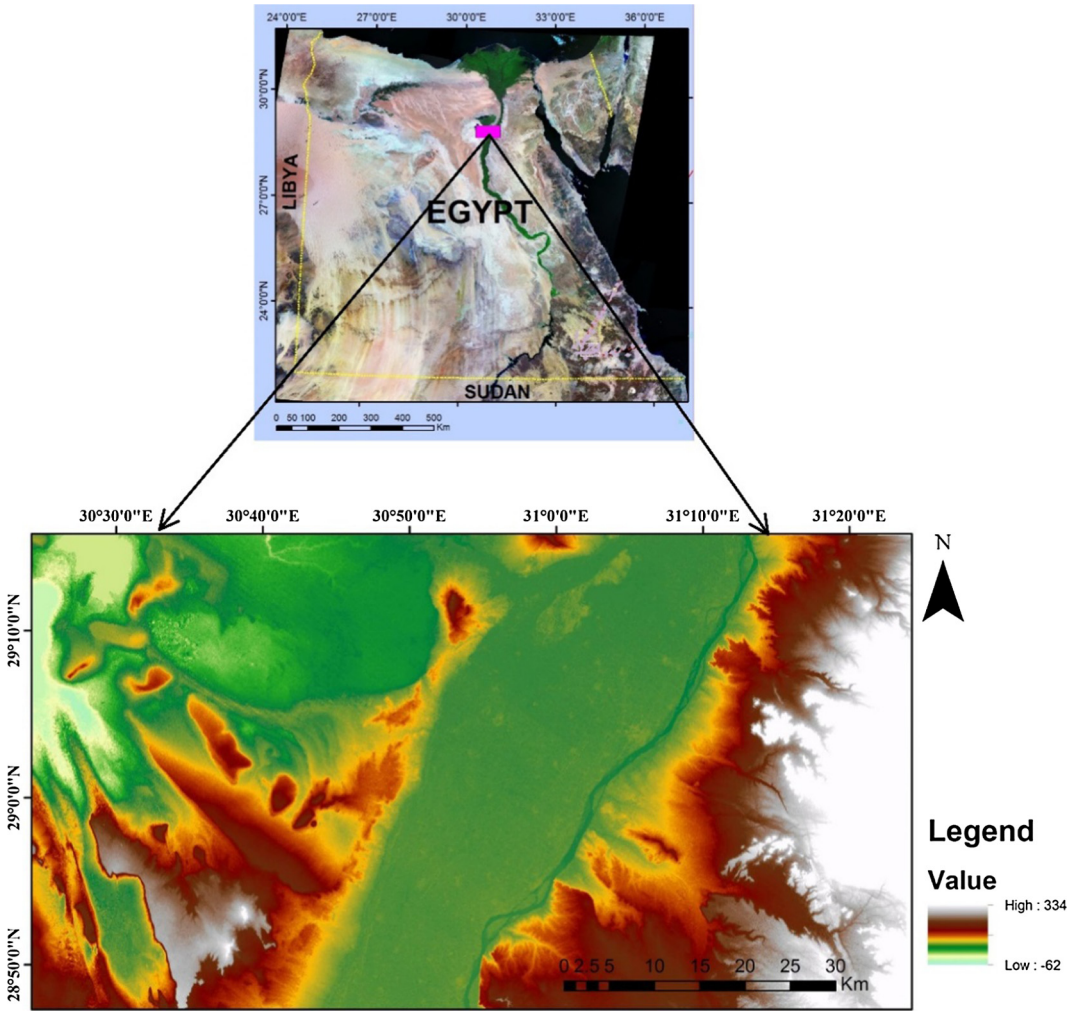

Figure 1 Location map of West Beni Suef area, Western Desert, Egypt.

The analog recorder was the two-channel Hewlett–Packard (HP-7130A) recorder, consisting of fine (10 nT full-scale) and coarse (100 nT full-scale) output traces, with separate fiducials (Aero-Service, 1984). Diurnal variation effects on the magnetic field, which arise due to solar activities, were recorded using an additional unit of the base station magnetometer (Varian VIW 2321 G4).

4. Data analysis and interpretation

The obtained data were corrected and plotted as total aeromagnetic intensity map. In this study, the digitizing process follows the basic acquired analog data flight lines drawn on the map and the obtained data are shown as filled colored map (Fig. 3). The aeromagnetic map of total intensity (Fig. 3) exhibits some high (red colored) and low (blue and green colored) anomalies, and reveals a prominent feature, as a circular and elongated shapes. These anomalies of major positive amplitude are called Agnes (red colored) and occupy two parts. The first part occupies the northern part of the map and consists of three anomalies. The second part is located at western part of the map and extends from NNW to SW part and includes fourth anomalies. However, the negative anomalies are located in many parts in the map of the study area and appear as elongated shapes and are colored with green and blue. The first anomaly is located at Middle Eastern part (blue colored). The second part occupied the southern part (blue colored). The third anomaly is located at central part and extends from north to south part (green colored). The fourth anomaly is located at northwestern corner of the map.

4.1. Qualitative interpretation of the airborne magnetic data

The qualitative interpretation of a magnetic map begins with a visual inspection of the shapes and trends of the major anomalies, and examination of the characteristic features of each individual anomaly, such as the relative locations and amplitudes of the positive and negative counterparts of the anomaly, the elongation and areal extent of the contours, as well as the sharpness of the anomaly. Therefore, the qualitative analysis is an attempt to have a preliminary idea about the characteristics of the causative bodies, depending on the form, shape, trend, differences in amplitude, changes or discontinuities of directions and extensions of anomalies (Nettleton, 1976).

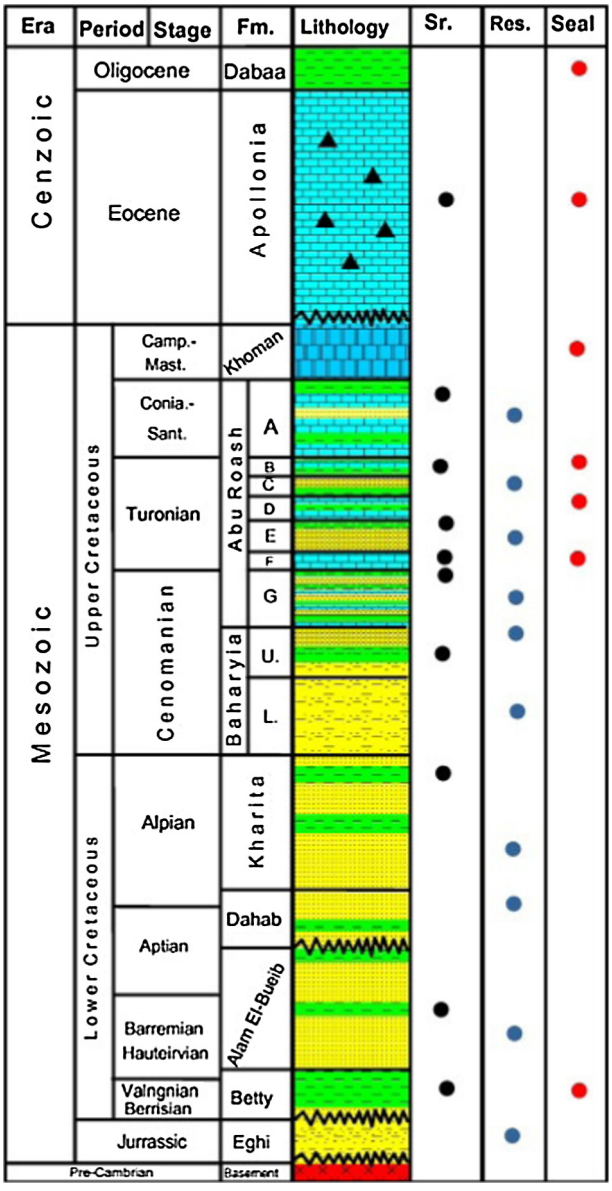

Figure 2 Subsurface geologic column of the Beni Suef Basin modified after (Zahran et al., 2011).

4.1.1. Reduction to the magnetic north pole

The total Intensity Magnetic Map (Fig. 3) is reduced to the northern magnetic pole RTP (Fig. 4) using Geosoft, Oasis Montaj software (Geosoft, 2007). This map reflects the northward shift in the positions of the inherited magnetic anomalies, due to the elimination of the inclination and declination of the magnetic field at this area; likewise, the sizes of the anomalies become larger and centered to some extent, over their respective causative bodies. In addition, the magnetic gradients became more intensive and steep, as well as the anomalies reliefs increase, giving rise to a higher resolution in the lithological and structural inferences encountered.

Several zones with high and low magnetic values are present; the magnetic highs are separated from magnetic lows by steep gradients. The elongations of magnetic gradients on the RTP map indicate that they are structurally-controlled by faults trending N-S and E-W directions. The high magnetic anomalies occupy two locations on the map. The first anomaly occupies nearly the eastern part of the area with N-S direction. It consists of four sub-anomalies with high magnitudes (red colored). The second high magnetic anomaly occupies the western corner.

Meanwhile, low magnetic anomalies occupy many locations of the map; the first anomaly occupies the eastern side. The second one occupies the middle southern part on the RTP map. The third anomaly is found in western part of the study area.

4.2. Quantitative interpretation of the ground magnetic data

The aims of any magnetic survey are to recognize the depth, position, shape and attitude of the responsible magnetic bodies in an area, and then interpret these values in terms of geological models which are consistent both with the observed geology and with the accepted geological theory (Boyd, 1969). The magnetic method is firmly established as an investigative procedure in applied geophysics and it is increasingly recognized as an understanding of the elements of magnetic petrophysics that assists in optimizing field data interpretation (Clark and Emerson, 1991).

4.2.1. Analysis of power spectrum transformation

The method of radial average power spectrum is used to determine the depths of volcanic intrusions, depths of the basement complex and the subsurface geological structures. Several authors, such as Bhattacharyya (1965), Spector and Grant (1970), Garcia and Ness (1994), and Maurizio et al. (1998), explain the spectral analysis technique based on the analysis of the magnetic data using the Fourier Transform. For this study, the Fast Fourier Transform (FFT) is applied on the RTP magnetic data, to calculate the energy spectrum.

The energy decay curve (Fig. 5) includes linear segments, with distinguishable slopes, that are attributed to the contributions in the magnetic data from the residual (shallower sources), as well as the regional (deep sources). The presentation of the method depends on plotting the energy spectrum against frequency on a logarithmic scale. Fig. 5 shows two different components as straight-line segments, which decrease in slope with increasing frequency. The slopes of the segments yield estimates of the average depths to magnetic sources.

The depth of each source ensemble responsible for each segment was calculated by introducing the slope of this segment in the formula:

$$H\ (\text{depth}) = -\text{slope}/4\pi \qquad (1)$$

The analysis of the power spectrum curve (Fig. 5) shows that, the deep seated magnetic component frequencies vary from 0 to 0.11 cycles/grid unit, while that of the near-surface magnetic component ranges from 0.11 to 0.36 cycles/grid unit. It revealed that, there are two main average levels (interfaces).

The estimated mean depths of both regional and residual sources are found to be 5.27 km and 2.79 km respectively.

4.2.2. Regional magnetic component

Usually in magnetic surveying, the local anomalies are of prime interest and first step in interpretation is the removal of the regional field to isolate the residual anomalies. The

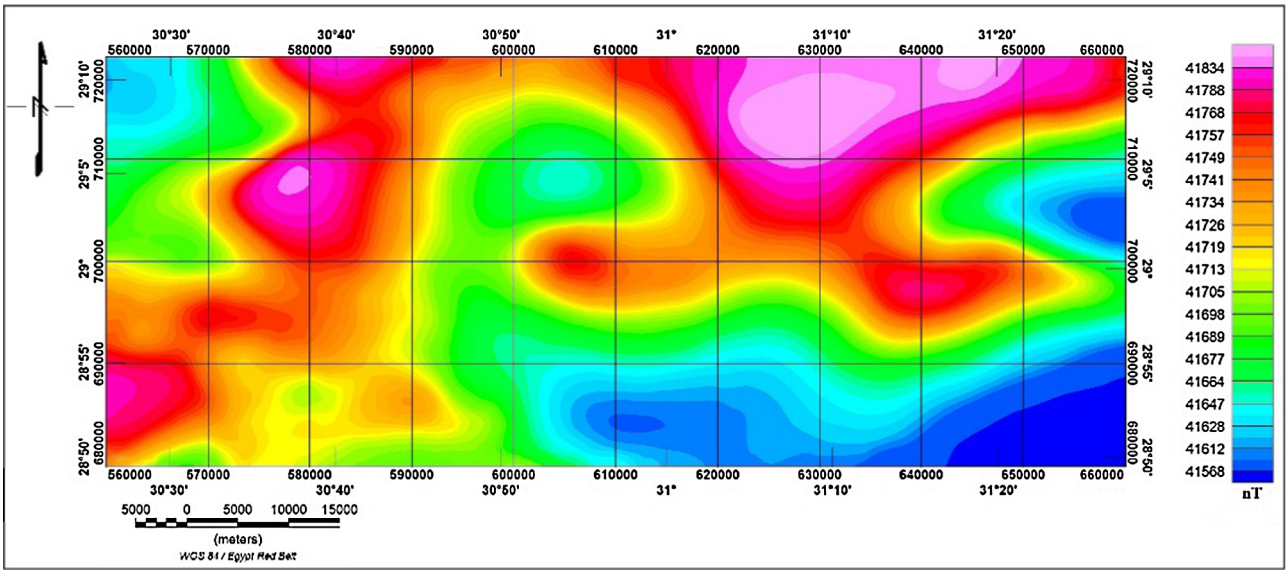

Figure 3 Total Intensity magnetic map of West Beni Suef area, Western Desert, Egypt.

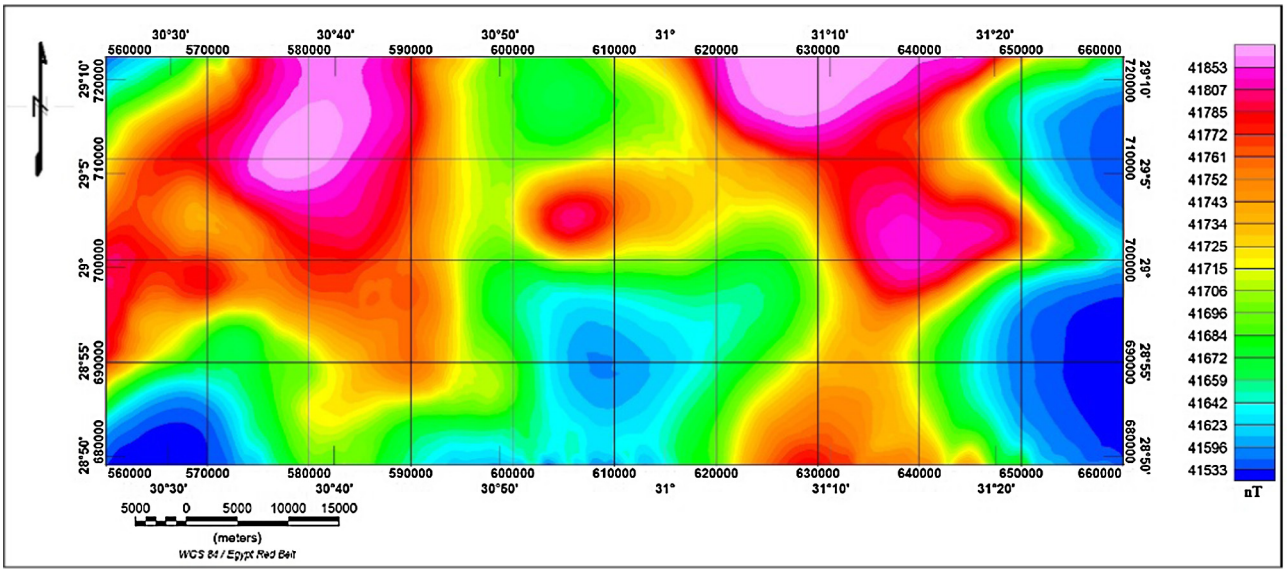

Figure 4 The reduced to the northern magnetic pole total intensity magnetic field (RTP) map of West Beni Suef area, Western Desert, Egypt.

technique, originally described by Griffin (1949), is the way of calculating the regional field and give satisfactory results.

Low-pass (regional) filtered map (Fig. 6) displays an increase in positive magnetic values (red colored) and occupied two parts on the map. The first part occupied nearly Eastern part and tack N-S direction and include four anomalies with high magnitude (red colored). The second part of high magnetic anomalies occupied the northwestern corner.

However, low regional magnetic anomalies (green and blue colored) occupy many parts on the map, the first occurrence occupied the eastern side. The second occurrence of low magnetic anomalies occupied the Sothern side on the regional map. The third occurrence found in center of northern part and extend from north to south side. The last anomaly of low magnetic anomaly appears as small anomaly and occupies the northwestern corner of the regional map.

4.2.3. Residual magnetic component

Residual maps have been used by geophysicists to bring into focus local features, which tend to be obscured by the broader features of the field (Ammar et al., 1988). The construction of residual maps is one of the best known ways of studying a potential map quantitatively, where the measured field includes effects from all bodies in the vicinity. The High-pass (residual) filtered map (Fig. 7) clearly shows several alternative negative (green and blue colored) and positive (red colored) magnetic anomalies. Some anomalies have elongated shapes, while others have semi circular shapes, which possess a general

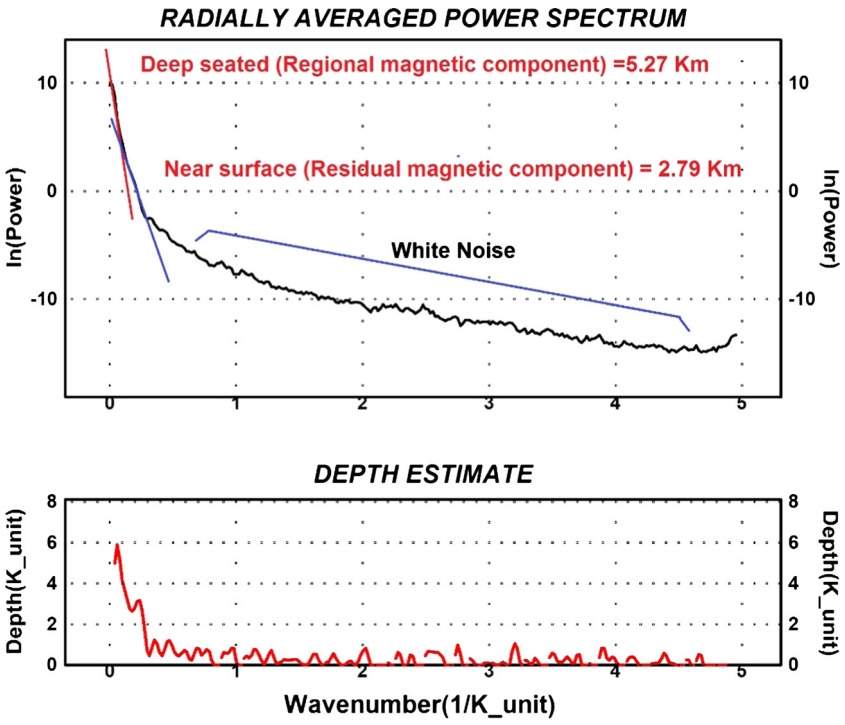

Figure 5 Radially averaged power spectrum and depth estimate of the RTP magnetic map of the West Beni Suef area, Western Desert, Egypt.

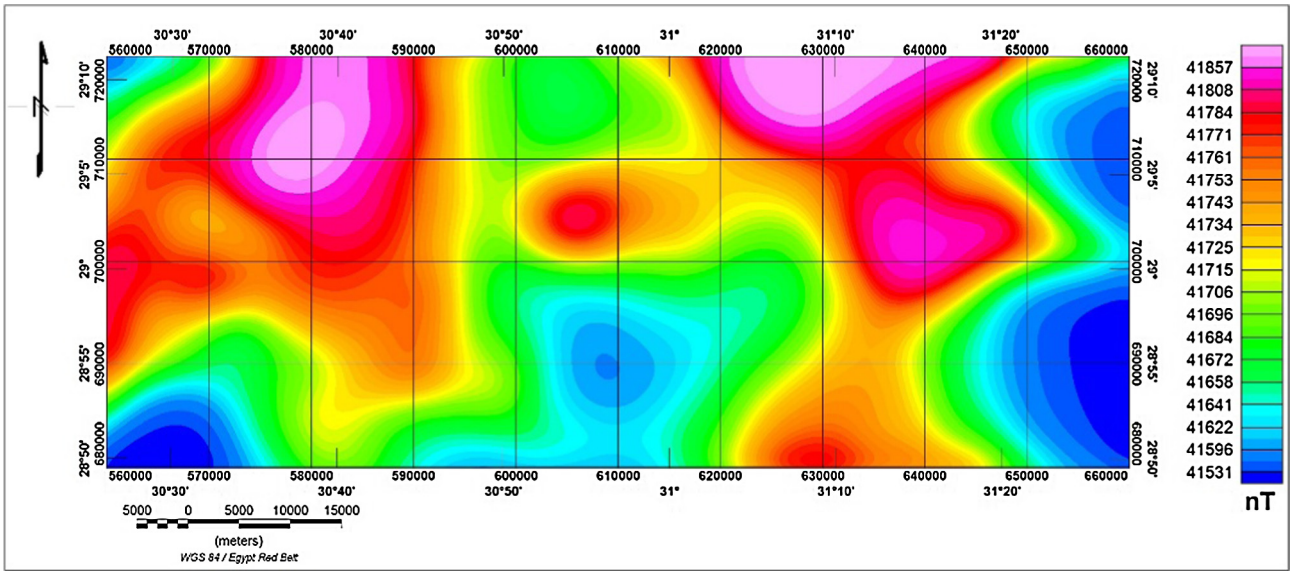

Figure 6 Regional (low-pass filtered) magnetic component of the RTP at West Beni Suef area, Western Desert, Egypt.

E-W, N-S and NNW-SSE directions. These zones are dissected by many faults in different directions. They may reflect different compositions of the basement rocks at the subsurface or shallow basins due to subsiding.

4.2.4. Euler deconvolution

Geophysical constraining is focused mainly on direct interpretation of the magnetic field by Euler deconvolution. The advantage of this method of magnetic data enhancement is that its amplitude function is always positive and does not need any assumption of the direction of body magnetization (Jeng et al., 2003). Euler deconvolution (Reid et al., 1990; Zhang et al., 2000) has come into wide use as an aid to interpreting profile or girded magnetic survey data. It provides automatic estimates of source location and depth. In doing this, it uses a structural index (SI) to characterize families of source types.

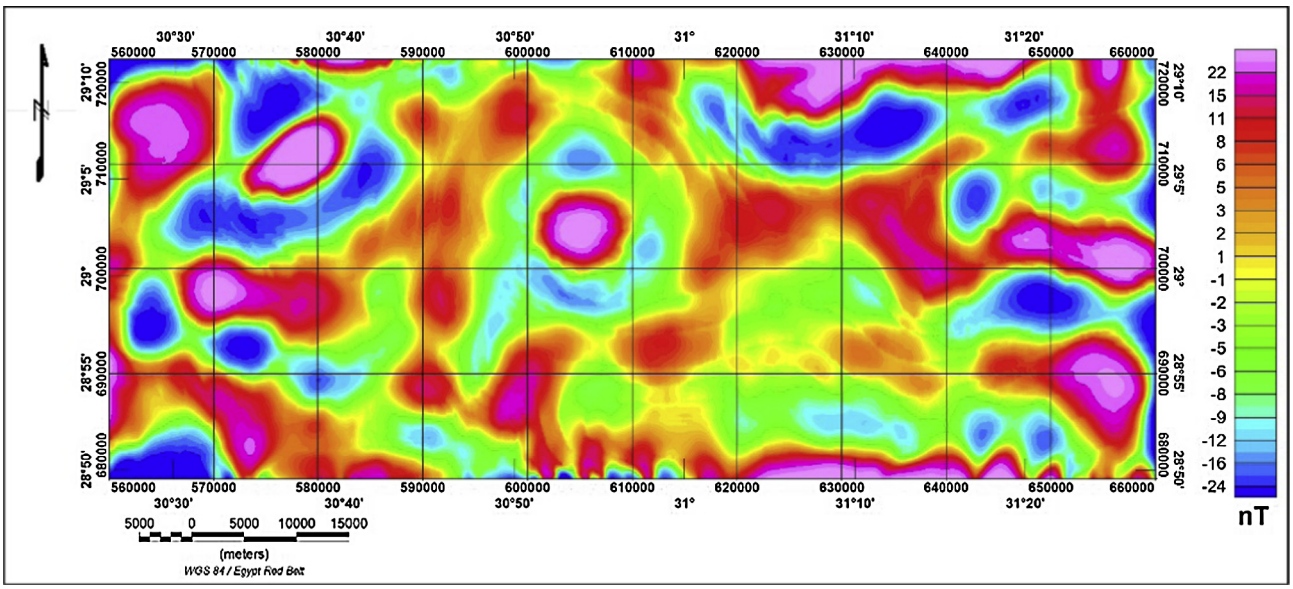

Figure 7 Residual (high-pass filtered) magnetic component of the RTP at West Beni Suef area, Western Desert, Egypt.

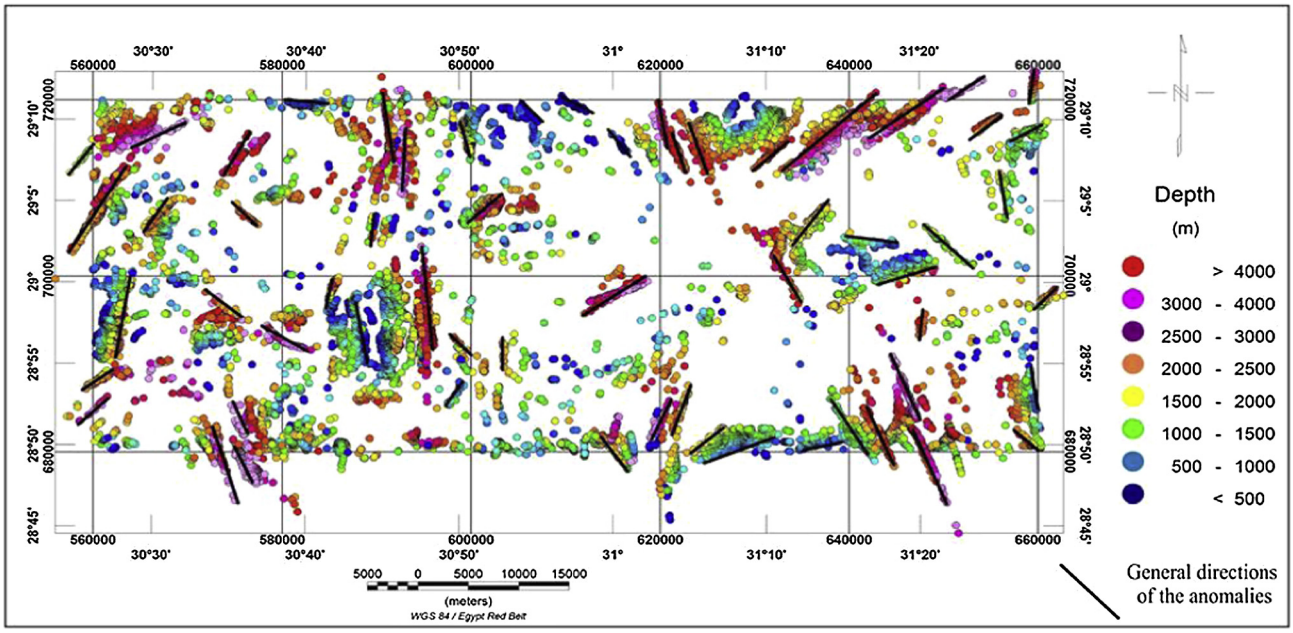

Figure 8 Depth to magnetic basement as calculated using Euler deconvolution (SI = 0) and the general directions of the anomalies at West Beni Suef area, Western Desert, Egypt.

In this investigation, Euler deconvolution technique has been carried out on the magnetic data using Geosoft (2007). Applying Euler deconvolution with SI = 0.0, an Euler map (Fig. 8) was derived which shows clustering of circles in linear shape indicating the nature of probable contacts between the rock units. The linear clustering circles are suggested to be the result of faults and or contacts with depth values ranging between 500 m and 4000 m. These solutions are trending in NW-SE, ENE-WSW, NE-SW, E-W and NNW-SSE directions (Fig. 8).

4.2.5. Trend analysis

Trend analysis is an extremely significant technique in the quantitative interpretation of all types of data either geology or geophysics. This method of analysis could reveal the directions (trends) of forces and their strengths, as well as mineralization may be emplaced and controlled.

The results of trend analysis generated from the application of rose diagram technique on the directions (trends) illustrated in Fig. 9 of the gradients and anomalies of the regional and residual magnetic trends are illustrated in (Fig. 8). These

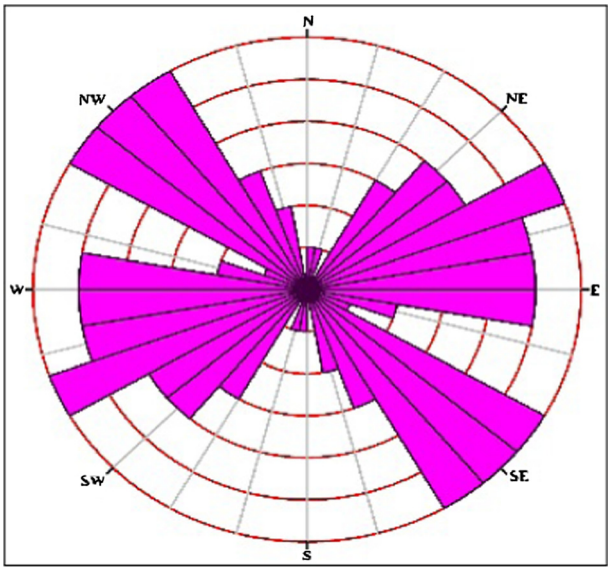

Figure 9 Rose diagrams showing the main structural lineaments as deduced from RTP map.

structure systems are statistically analyzed and plotted in the form of rose diagrams as shown in Fig. 9. The examination of these diagrams shows four predominant structural trends having variable intensities and lengths. These are the NW, NE, ENE, and E–W trends, representing the most predominant tectonic trends affecting the investigated area as deduced from the magnetic point of view. However, the other minor structural trends appearing on the rose diagrams such as the N–S, NNE and NNW, are of less significance in this area. The structural lineaments at shallow and deep depths of the prospect area were interpreted from the RTP map. Statistical trend analysis is achieved here for the resolution of the azimuths of the outlined interpreted lineaments. Rose diagrams were constructed for the interpreted structural lineaments in order to assist in defining the principal structural trends in the prospect area of study.

4.2.6. 2D magnetic modeling

Six magnetic profiles (Fig. 10) are modeled using the 2D modeling technique. The RTP magnetic values along these profiles have been traced.

Using the available geologic information, the previously carried out magnetic depth determinations, and the results of qualitative interpretation of magnetic maps; basement structural cross-sections are constructed along these profiles to initiate modeling. The magnetic susceptibility contrast values have been assumed. The magnetic field was calculated iteratively for the assumed geologic model, until a good fit is reached between the observed and calculated profiles.

The modeled profiles are shown in Figs. 11–16. The observed RTP magnetic profile is shown as a black circle on the upper half of the model, while the calculated magnetic data are drawn as solid black profile superimposed on the observed RTP data. The degree of error is plotted also, in the upper half of the model, as red line. The lower half of the model shows the assumed cross section. The horizontal *x*-axis represents the horizontal distance, in kilometers, along the profile. The vertical axis shows two different parts. The upper part represents the magnetic anomaly scale, in (nT) unit, and the lower part represents the depth scales, in meters. Therefore, the upper half of the graph shows, both the observed and the calculated profiles as well as the degree of error, while the lower half of the graph represents the modeled basement structure.

The first profile lies in the northern part of the study area and has direction W-E and denoted as P1 (Fig. 10). Close examination of this profile shows an excellent fit between the observed and calculated anomalies with error reaches 1.517 (Fig. 11). This model consists of three blocks which reflect composition variations of basement. Also, the model reflects the presence of basinal area affecting the basement in the

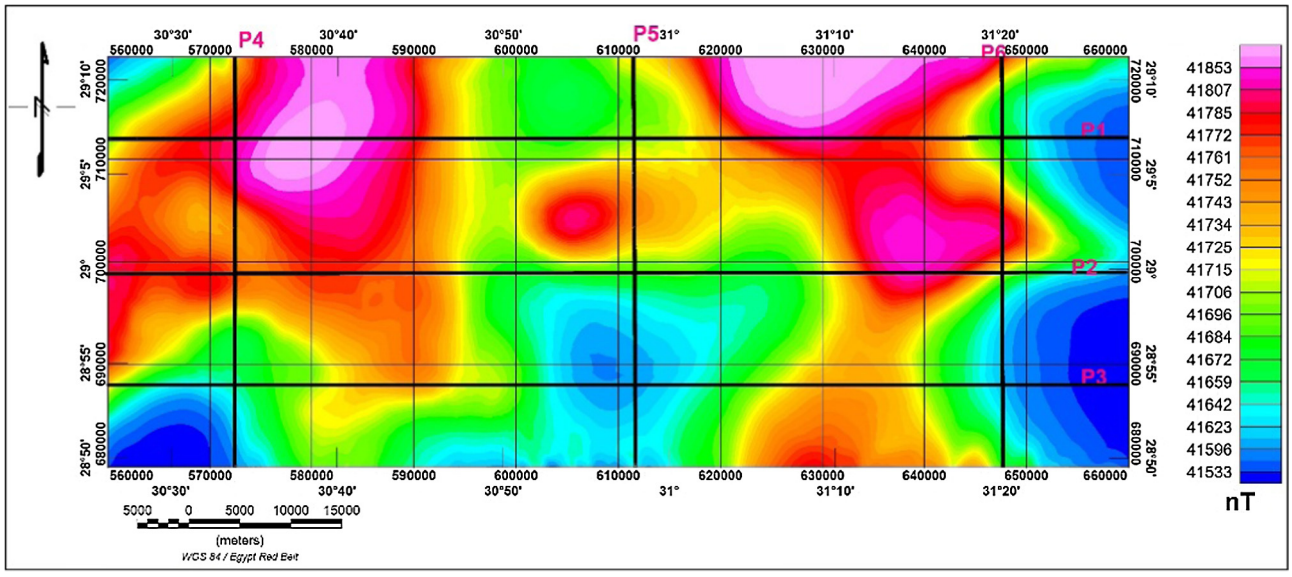

Figure 10 The distribution of six profiles on RTP magnetic map.

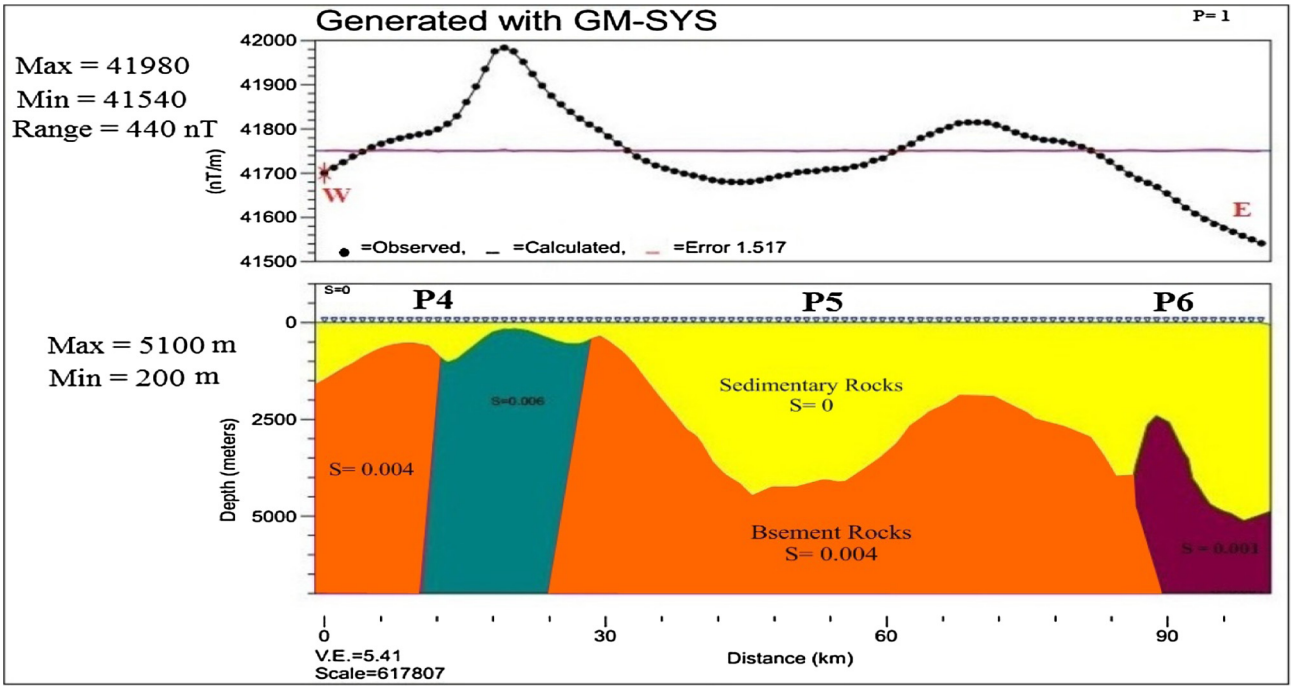

Figure 11 Two - dimensional (2D) modeled magnetic Profile 1, West Beni Suef area, Western Desert, Egypt.

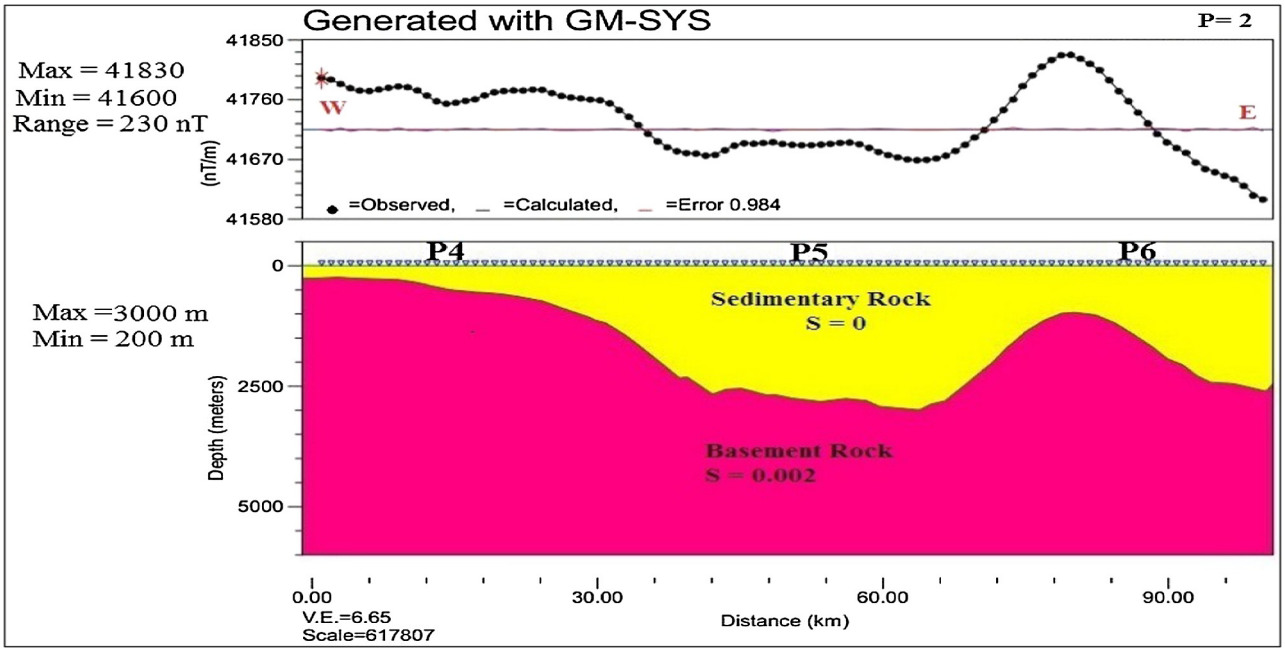

Figure 12 Two - dimensional (2D) modeled magnetic profile 2, West Beni Suef area, Western Desert, Egypt.

central part of the model reaching depth of about 4500 m. The basement depth along the profile ranges between 200 and 5100 m.

The second profile lies in the middle part of the study area and denoted as P2 (Fig. 10). This profile P2 is going from the West to the East direction. Close examination of this profile shows an excellent fit between the observed and calculated anomalies with error reaches 0.984 nT (Fig. 12). This profile shows a homogeneous basement. The basement depth along the profile ranges between 200 and 3000 m.

The third profile lies in the southern part of the study area and denoted as P3 (Fig. 10). This profile P3 is going from the West to the East direction. Close examination of this profile shows an excellent fit between the observed and calculated anomalies with error reaches 1.259 nT (Fig. 13). The basement indicates a range of depths oscillating between 250 and 6000 m.

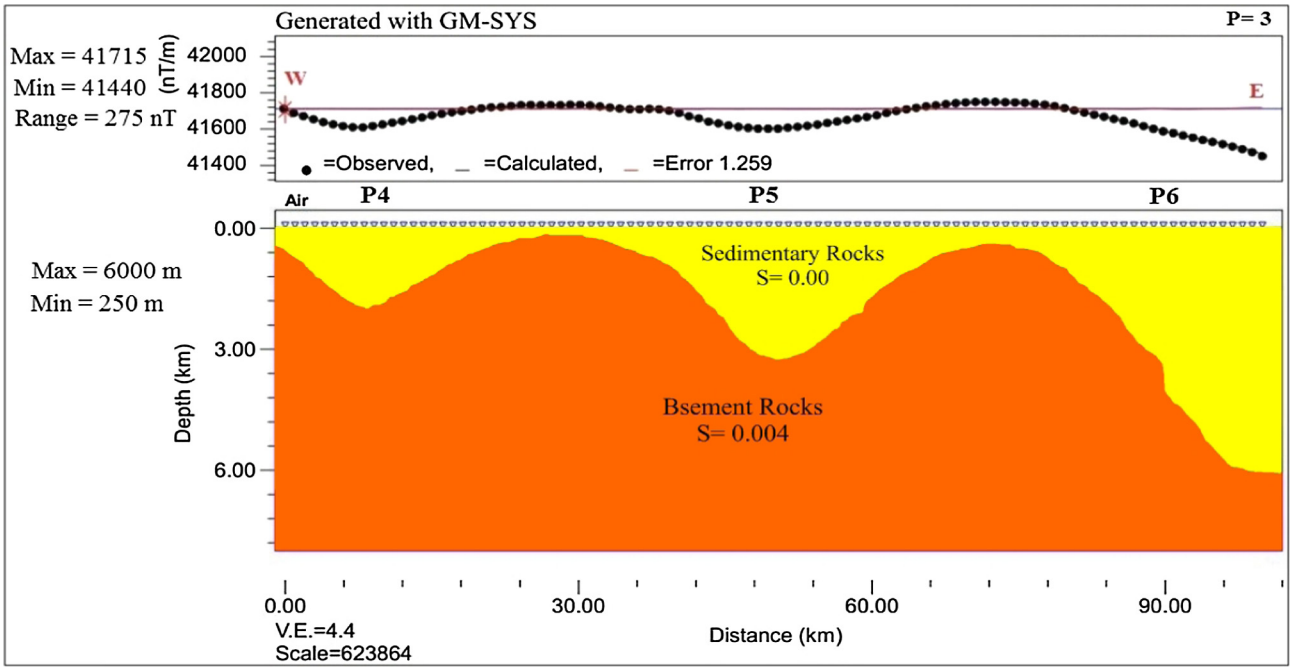

Figure 13 Two - dimensional (2D) modeled magnetic profile 3, West Beni Suef area, Western Desert, Egypt.

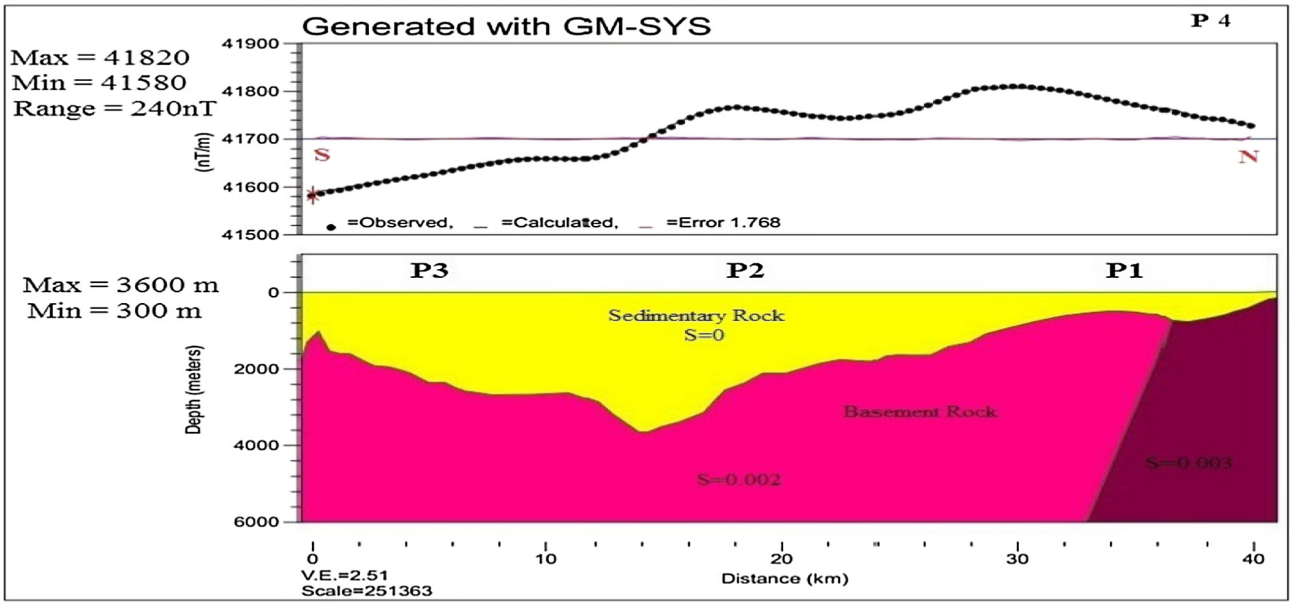

Figure 14 Two - dimensional (2D) modeled magnetic profile 4, West Beni Suef area, Western Desert, Egypt.

The fourth profile lies in the western part of the study area and denoted as P4 (Fig. 10). This profile P4 is going from the South to the North direction. Close examination of this profile shows an excellent fit between the observed and calculated anomalies with error reaches 1.768 nT (Fig. 14). There are two blocks with different composition. The formed basement indicates a range of depths varying between 300 and 3600 m.

The fifth profile lies in the central part of the study area and denoted as P5 (Fig. 10). This profile P5 is going from the South to the North direction. Close examination of this profile shows an excellent fit between the observed and calculated anomalies with error reaches 0.785 nT (Fig. 15). There are two blocks with varying compositions forming the basement. The basement depths are varying from 500 to 3800 m.

The sixth profile lies in the eastern part of the study area and denoted as P6 (Fig. 10). This profile P6 is going from the South to the North direction. Close examination of this profile shows an excellent fit between the observed and calculated anomalies with error reaches 1.278 nT (Fig. 16). There are two blocks representing the basement. The basement depths are ranging between 850 and 4000 m.

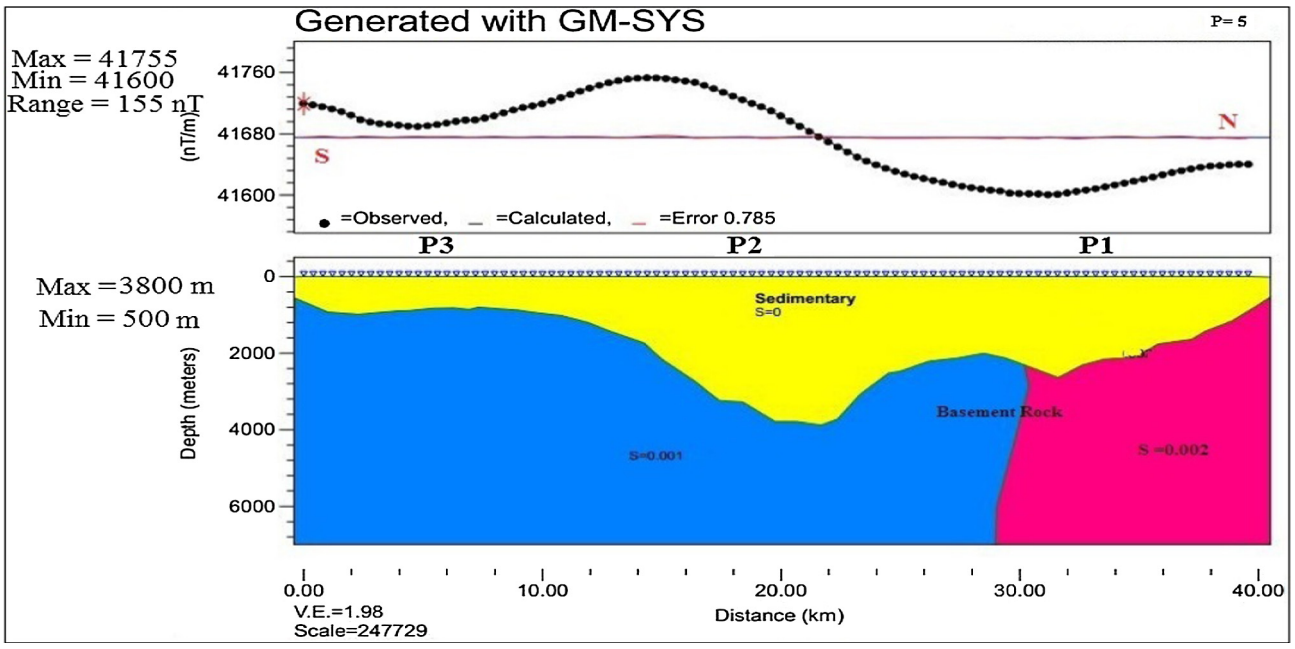

Figure 15 Two - dimensional (2D) modeled magnetic profile 5, West Beni Suef area, Western Desert, Egypt.

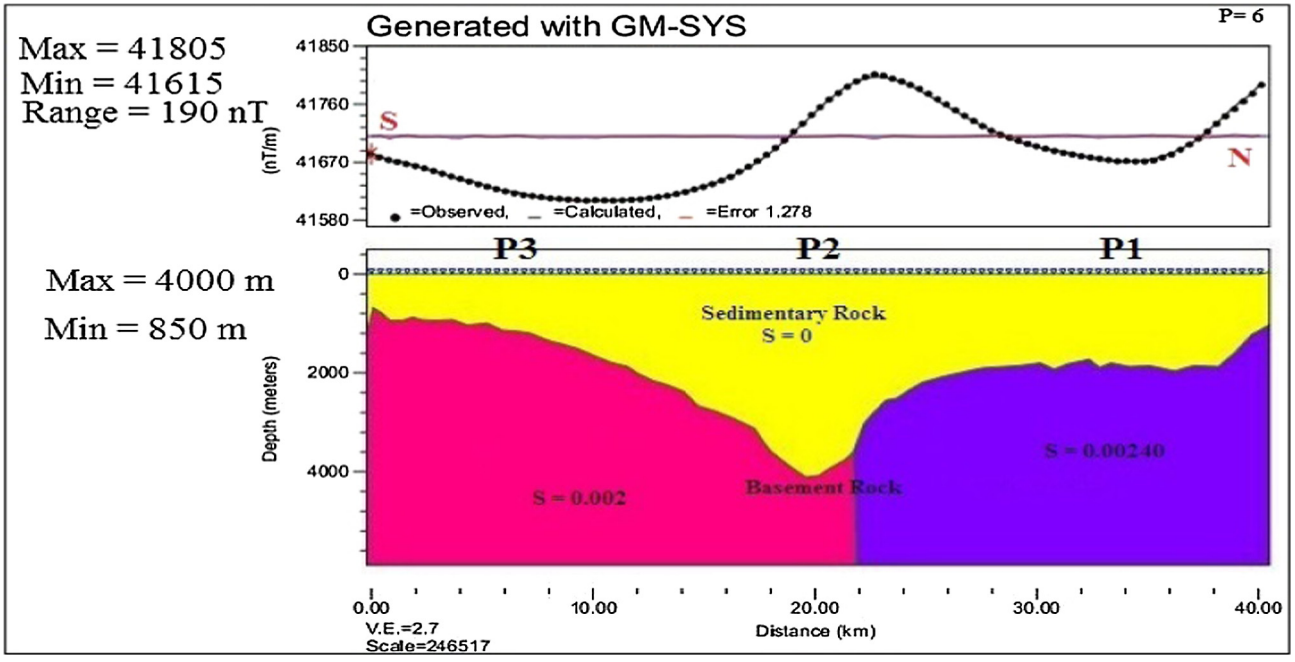

Figure 16 Two - dimensional (2D) modeled magnetic profile 6, West Beni Suef Area, Western Desert, Egypt.

As a conclusion derived from these models, we can conclude that the basement rocks in the study area are varying in their composition as reflected by the range of magnetic susceptibility (0.001–0.006 c.g.s unit) assigned for the different blocks. The basement depth is varying and has value ranging between 200 and 6000 m.

4.2.7. Depth of basement

The locations of these profiles are illustrated on RTP map (Fig. 10). In addition, the depths of the basement surface are digitized and used to construct the basement depth map. The interpreted basement depth map (Fig. 17) shows that the northern and eastern parts of the basement is deeper than the western and southern parts (trough). The basement depth in these areas reaches to 5095 m. In the southern and western parts of the study area, the basement depth reaches to 246 m (swells). According to this map we conclude that the larger sedimentary thickness will be found in the eastern and northern parts of the study area while the lowest sedimentary thickness will be found in the western part.

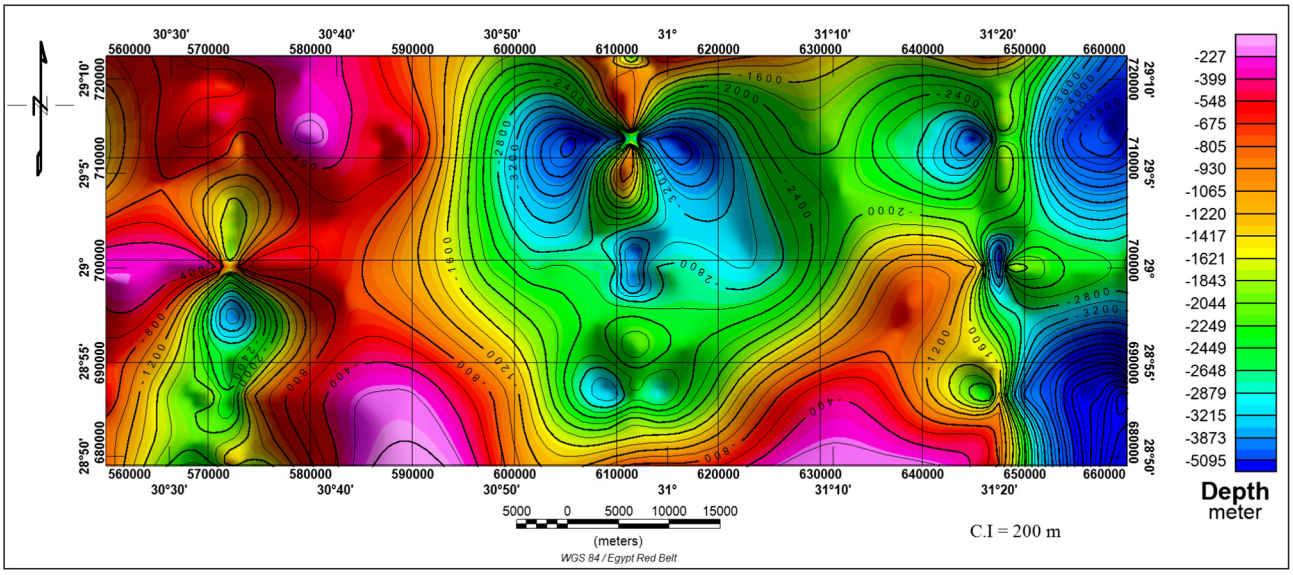

Figure 17 Basement depth map at Beni Suef area, Western Desert, Egypt.

5. Summary and conclusions

From the present study, we can conclude that:

The total Intensity Magnetic Map is reduced to the northern magnetic pole (RTP. The regional – residual separation is applied on the reduce to magnetic pole map. The analysis of the power spectrum curve shows that, the deep seated magnetic component frequencies vary from 0 to 0.11 cycles/grid unit, while the near-surface magnetic component ranges from 0.11 to 0.36 cycles/grid unit. The estimated mean depths of both regional and residual sources are found to be 5.27 km and 2.78 km respectively. Euler deconvolution is applied to illustrate the distribution of faults and to estimate their depths. It shows faults running in the NW-SE, ENE-WSW, NE-SW, E-W and NNW-SSE directions, and the fault depths are ranging from 500 to 4500 m. Depths to the basement surface are calculated along six profiles covering almost the study area, using 2-D modeling technique. The depth of basement surface reaches to 5095 m in the northern and eastern parts of the study area, while it reaches 227 m in the southern and western parts.

References

Abu El-Ata, A.S., 1990. The role of seismic-tectonics in establishing the structural foundation and saturation conditions of El-Gindi basin, Western Desert, Egypt. In: Proc. of the 8th Ann. Meet. EGS (Egyptian Geophysical Society), pp. 150–189.

Aero-Service, 1984. Final operational report of airborne magnetic/radiation survey in the Eastern Desert, Egypt. For the Egyptian General Petroleum Corporation (EGPC) and the Egyptian Geological Survey and Mining Authority (EGSMA), Aero-Service Division, Houston, Texas, USA, Six Volumes.

Ammar, A.A., Fouad, K.M., Meleik, M.L., 1988. In: Evaluation of the Efficiency of Shortend Low-Pass Filters Computed by Inverse Fourier Transform for Potential Fields of Spherical Bodies and Planar Regionals, vol. 1. Faculty of Earth Sciences, King Abdulaziz University, Jeddah, pp. 133–148.

Bhattacharyya, B.K., 1965. Two-dimensional harmonic analysis as a tool for magnetic interpretation. Geophysics 30, 829–857.

Boyd, D., 1969. The contribution of airborne magnetic surveys to geological mapping. In: Mining and Ground Water Geophysics. Geol. Surv. of Canada, pp. 213–227, Economic Geology Report No. 26.

Clark, D.A., Emerson, D.W., 1991. Notes on rock magnetization characteristics in applied geophysics studies. Explor. Geophys. 22, 547–555.

Domzalski, W., 1966. Importance of aeromagnetics in evaluation of structural control of mineralization. Geophys. Prospect. XIV (3), 273–291.

Garcia, J.G., Ness, G.E., 1994. Inversion of the power spectrum from magnetic anomalies. Geophysics 59 (3), 391–401.

Geosoft, 2007. Geosoft mapping and application system Inc, Suit 500, Richmond St. West Toronto, ON Canada N5SIV6.

Griffin, W.R., 1949. Residual gravity in theory and practice. Geophysics 14, 39.

Hantar, G., 1990. North western desert. In: Said, R. (Ed.), The Geology of Egypt. AA Balkema, Rotterdam, pp. 293–319.

Jeng, Y., Lee, Y.L., Chen, C.Y., Lin, M.J., 2003. Integrated signal enhancements in magnetic investigation in archaeology. J. Appl. Geophys. 53, 31–48.

Maurizio, F., Tatina, Q., Angelo, S., 1998. Exploration of a lignite bearing in Northern Ireland, using ground magnetic. Geophysics 62 (4), 1143–1150.

Meshref, W., Abdel, Baki S., Abdel, Hady H., Soliman, S., 1980. Magnetic trend analysis in the northern Arabian Nubian Shield and its tectonic implications. Ann. Geol. Surv. Egypt 10, 939–953.

Meshref, W.M., 1982. Regional structural setting of north Egypt. In: E.G.P.C.; The 6th Exploration and Production Conf., Cairo, p. 18.

Nettleton, L.L., 1976. Gravity and Magnetic in Oil Prospecting. McGraw-Hill Book Co., Inc., New York, p. 464.

Reid, A.B., Allsop, J.M., Ganger, H., Millett, A.J., Somerton, I.w., 1990. Magnetic interpretation in three dimensions using Euler deconvolution. Geophysics 55, 80–91.

Riad, S., 1977. Shear zones in the north Egypt, interpreted from gravity data. Geophysics 42 (6), 1207–1214.

Said, R., 1962. The Geology of Egypt. Elsevier Publ. Co., Amsterdam. Oxford and New York.

Spector, A., Grant, F.S., 1970. Statistical models for interpreting aeromagnetic data. Geophysics 35, 293–302.
Weeks, G., 1952. Factors of sedimentary basin development that control oil occurrence. Am. Assoc. Pet. Geol. Bull. 37, 2071–2124.
Zahran, H., Abu Elyazid, k., El-Aswany, M., 2011. Beni Suef Basin the key for exploration future success in Upper Egypt. In: AAPG Annual Convention and Exhibition, Houston, Texas, USA, April 10–13, 2011.
Zhang, C., Mushayandebvu, M.F., Reid, A.B., Fairhead, J.D., Odegard, M.E., 2000. Euler deconvolution of gravity tensor gradient data. Geophysics 65, 512–520.